Comparison of different Kalman filter approaches in deriving Time Varying Connectivity from EEG data

Eshwar Ghumare[1], Maarten Schrooten[2], Rik Vandenberghe[2] and Patrick Dupont[3]

***Abstract*— Kalman filter approaches are widely applied to derive time varying effective connectivity from electroencephalographic (EEG) data. For multi-trial data, a classical Kalman filter (CKF) designed for the estimation of single trial data, can be implemented by trial-averaging the data or by averaging single trial estimates. A general linear Kalman filter (GLKF) provides an extension for multi-trial data. In this work, we studied the performance of the different Kalman filtering approaches for different values of signal-to-noise ratio (SNR), number of trials and number of EEG channels. We used a simulated model from which we calculated scalp recordings. From these recordings, we estimated cortical sources. Multivariate autoregressive model parameters and partial directed coherence was calculated for these estimated sources and compared with the ground-truth. The results showed an overall superior performance of GLKF except for low levels of SNR and number of trials.**

I. INTRODUCTION

Effective or directed connectivity is receiving increased attention for exploring the information processing in the human brain [1]–[3]. Unlike functional connectivity, effective connectivity allows to study the information flow and interaction timings among brain regions to understand the basis of cognitive functions. In contrast to functional magnetic resonance imaging (fMRI), data from electroencephalography (EEG) has an excellent time resolution. Using such data, we can study the effective connectivity to understand the spectral as well as the temporal properties of these directed connections. Among the different approaches proposed for effective connectivity analysis, Multivariate Autoregressive Modeling (MVAR) based on the concept of Granger causality (GC) is widely applied [2]. GC based MVAR measures give directed flow by estimating a linear causal relationship among brain regions. In this article, we focused on partial directed coherence (PDC), one of the commonly applied GC based frequency domain measures.

The estimation of PDC follows the multivariate autoregressive (MVAR) modeling of the EEG time series. The estimated MVAR parameters are transformed to the frequency domain to calculate PDC values. Among all MVAR estimation approaches, a Kalman filter based MVAR modeling gained wider applications due to its accurate estimation of non-stationary and high dimensional EEG data [4], [5]. Kalman filter based approaches are able to best follow transient changes in spectra of EEG data and give estimates of the MVAR model at each time point, i.e. time varying MVAR (TV-MVAR). Hence time varying PDC (TV-PDC) can be calculated.

A Kalman filter can be implemented by a number of ways to estimate the TV-MVAR model. The classical Kalman filter (CKF) based approach can be used in case of single trial EEG or averaged event related potential (ERP) data [6]. An alternative is to use the EEG of the individual trials by estimating the TV-MVAR model of each single trial and by averaging the model estimates across trials followed by TV-PDC calculation [7]. A third approach is to calculate TV-PDC from the TV-MVAR estimates of each single trial and the final TV-PDC is obtained by averaging TV-PDC across trials [8], [9]. The General Linear Kalman filter (GLKF) provides an extension of CKF to the case of multi-trial time series [4]. GLKF based estimation allows the simultaneous fit of one MVAR model to all trials. For multi-trial EEG data, GLKF is considered to be more effective to estimate the TV-MVAR model [10]. However, to the best of our knowledge, no study directly comparing the accuracies of the different strategies is available.

The performance of GLKF was studied for different levels of signal to noise ratio (SNR) and number of trials [11], [12]. A high number of trials is important to accurately estimate the model and to increase the adaptation speed (i.e. the speed of change of MVAR estimates to minimize prediction error). The SNR is an another factor which may strongly influence the reliability of the approach. Although several papers have investigated the accuracy of GLKF [11], [12], none have compared CKF and GLKF approaches directly at different levels of trials and SNR.

II. METHODS

A. Theoretical Background

1) Time varying MVAR (TV-MVAR): The time varying MVAR (TV-MVAR) process is described as:

$$Y(t) = \sum_{k=1}^{p} A(k,t)\ Y(t-k) + U(t) \qquad (1)$$

where $Y(t)$ is the set of time series, p is the model order, $A(k,t)$ is the matrix of time varying model parameters at time t for lag k =1, 2..., p and $U(t)$ is a vector of multivariate zero-mean uncorrelated white noise.

[1]Eshwar Ghumare (eshwar.ghumare@med.kuleuven.be) is with the Laboratory for Cognitive Neurology, Department of Neurosciences, KU Leuven, Leuven, Belgium.

[2]Maarten Schrooten and Rik Vandenberghe are with the Laboratory for Cognitive Neurology, Department of Neurosciences, KU Leuven, Leuven, Belgium and the Neurology Department, University Hospitals Leuven, Leuven, Belgium.

[3]Patrick Dupont (patrick.dupont@med.kuleuven.be) is with the Laboratory for Cognitive Neurology, Department of Neurosciences, KU Leuven, Leuven, Belgium and the Medical Imaging Research Center (MIRC), KU Leuven, Leuven, Belgium.

978-1-4244-9270-1/15/$31.00 ©2015 IEEE

2) Time varying Partial directed coherence (TV-PDC): Partial directed coherence (PDC) is a full multivariate spectral measure based on the concept of Granger causality (GC) [13], used to determine the directed influences between a pair of time series with the influence of the remaining time series removed. Using TV-MVAR parameters, we can obtain time varying PDC (TV-PDC) values. TV-PDC from node j to node i is calculated as a function of frequency and time as:

$$\pi_{ij}(f,t) = \frac{\bar{A}_{ij}(f,t)}{\sqrt{\sum_{r=1}^{m} \bar{A}_{rj}(f,t)\ \bar{A}^{H}_{rj}(f,t)}}, \ \sum_{i} |\pi_{ij}(f,t)|^2 = 1 \quad (2)$$

in which the superscript H stands for the Hermitian transpose and

$$\bar{A}(f,t) = I - \sum_{k=1}^{p} A(k,t) e^{-i2\pi fk} \quad (3)$$

where f is the normalized frequency in the interval [-.5,.5]. We used the squared values of PDC i.e. $|\pi_{ij}(f,t)|^2$ as measure of connectivity. Squared values of PDC were shown to provide superior accuracy than PDC [14].

3) TV-MVAR model estimation using Kalman filtering: A Kalman algorithm is applied in a linear state-space representation of the signal model. The linear state equation can be represented as:

$$A(k,t) = A(k,t-1) + V(k,t-1) \quad (4)$$

where *A(k,t)* is the state process i.e. TV-MVAR model parameters and *V(k,t)* is the additive noise in the state process. The measurement equation is given by (1).

The Classical Kalman filter(CKF) approach models single trial EEG/ERP data. Details of this algorithm are described in [4], [15]. For multi-trial data we implemented the following 3 strategies to estimate TV-PDC.

(1) TV-PDC is calculated from the averaged TV-MVAR estimates (CKF-AA) [7].

(2) TV-PDC is obtained by averaging TV-PDC across trials (CKF-PA) [8], [9].

(3) CKF applied to the average of all trials (CKF-GA) [6]

The algorithm was implemented using the *mvaar.m* function available from the Time series analysis toolbox [16].

The fourth strategy was General linear Kalman filter (GLKF) which was implemented in MATLAB as described in [5].

B. Simulated data

We used simulated data to compare the different approaches at various levels of SNR, number of trials and number of EEG channels. We defined a ground-truth model at the level of cortical sources. Based on this model, we simulated EEG scalp recordings. We linearly inverse estimated the cortical sources using Brainstorm (v3.2). The estimated sources were compared with the ground-truth model.

1) Simulated cortical connectivity model: The ground-truth model we used is based upon a model described in a previous simulation study [11] modified by adding a feedback connection to test the performance of the different approaches in the presence of a feedback connection. The simulated connectivity pattern consisted of 3 nodes or time series with a predefined linear causal TV-MVAR structure as depicted in Fig.1.

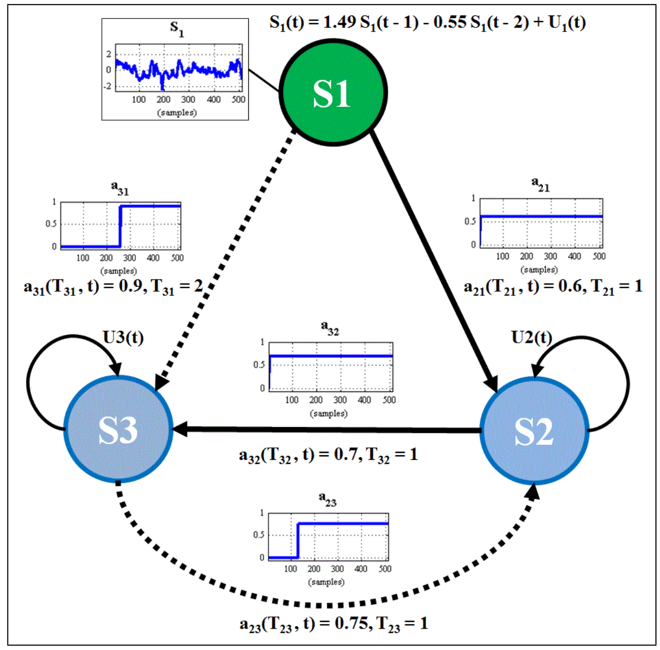

Fig. 1. Connectivity pattern imposed among 3 nodes. The value of the causal connection from S1→ S3 and S3→ S2 are time dependent (dotted arrow) and constant for the rest (continuous arrow). The theoretical (simulated) values are represented by the blue plots near each connection for the time lag given by T_{ij} (representing the constant delay in the propagation from node j to node i). For the other time lags, $a_{ij} = 0$. A time lag of 1 and 2 correspond to 4 and 8 ms, respectively.

To obtain simulated test signals similar to real cortical sources, the input time series for node S1 was generated from auto regression (AR) parameters estimated from a real cortical source which was estimated from a real EEG recording using Brainstorm [17]. The AR parameters of signal S1 are shown in Fig.1.

The remaining two signals were generated using TV-MVAR modeling (Fig.1). Values of $U_j(t)$ were adjusted at each time point or sample to achieve the SNR level of 10. The model was constructed iteratively in time using the model in Fig.1 to generate single trial data. We repeated the procedure to obtain 40 trials. The sampling frequency of the signal (Fs) was set to 256 Hz and the total number of time points (N) was set to 512 corresponding to two seconds recording.

2) Simulated EEG recordings: We assigned the simulated data in the three nodes of the model to 3 different cortical surface vertices modeled as current dipoles using the default anatomy in Brainstorm. We positioned the dipoles in the following Montreal neurological institute (MNI) coordinates (32, 108, 8), (33, 73, 56) and (66, 48, 20) for S_1, S_2 and S_3, respectively. We choose the coordinates based on previous studies on visuospatial attention from our lab [18]. EEG channel files for different number of channels (32, 64, 128 and 256) from ANT Neuro sensors were used. The forward matrix (G) was estimated for each channel file with the symmetric Boundary Element Method [19] implemented in Brainstorm. EEG scalp signals were calculated with an average reference. The forward matrix of each EEG channel file was used to simulate EEG data from the 3 simulated cortical sources *S(t)*. Corresponding EEG recordings were generated using Brainstorm for each EEG channel file and each trial of *S(t)* to generate multi-trial EEG data. White noise was added on the simulated EEG data. SNR was defined as the ratio of global power in the EEG recordings to variance of white noise added [20].

3) Source Modeling: The diagonal noise covariance of the EEG data required for the inverse estimation was calculated from EEG data in each trial separately using the complete two second recording of the trial. For each trial, the solution of the inversion kernel was achieved using the sLORETA (standardized low resolution brain electromagnetic tomography) method implemented in Brainstorm [21]. We used the default settings in Brainstorm to perform the source modeling. The orientations of the estimated dipoles are normal to the cortical surface. The time series of the reconstructed sources was taken as the cortical activity of the vertex point corresponding to the original source position.

4) TV-MVAR estimation defaults: The Kalman filter control parameters, also referred as update constant and which control the adaptation speed of MVAR parameters, were set to 0.02 [11], [20]. We estimated the model order by fitting a stationary MVAR model to the simulated data using the ARFIT algorithm from the Time series analysis toolbox [16], [22]. As criterion we used Schwarz's Bayesian Criterion because it is least affected by the presence of noise [23]. In this study, we found model order 3.

C. Performance analysis

1) Factors and levels: The SNR of the surface EEG, the number of trials and the number of EEG channels were chosen as factors to vary to test the performances. We used SNR = [0.1, 1, 3, 5, 10], number of trials = [1, 2, 3, 5, 10, 20, 40] and number of EEG channels = [32, 64, 128, 256]. We used 50 noise realizations for each setting.

2) Theoretical TV-PDC: We constructed the theoretical TV-PDC [11]. We limited our analysis within the frequencies 0-30 Hz based on the spectral power of the signal assigned to node S1.

3) Figures of merit: We used two figures of merit to capture the performance of each method at the level of detecting the TV-MVAR model parameters a_{ij} and at the level of TV-PDC. First, we used the mean square error (MSE) between the theoretical and estimated TV-MVAR parameters (denoted as $\mathrm{MVAR_{fom}}$) and second the MSE between the theoretical and estimated TV-PDC values (denoted as $\mathrm{PDC_{fom}}$). The diagonal elements were excluded from the calculation of $\mathrm{PDC_{fom}}$ due to the column normalization properties of PDC.

4) Statistical testing: We performed separate one-way repeated measures ANOVAs for $\mathrm{MVAR_{fom}}$ and $\mathrm{PDC_{fom}}$ as dependent variable to compare the four Kalman filter based approaches. This was done for each combination of SNR, number of trials and number of EEG channels. A Greenhouse - Geisser correction for sphericity was used. The post-hoc analysis was performed with the Scheffé's test. Statistical significance was set at $p < 0.05$.

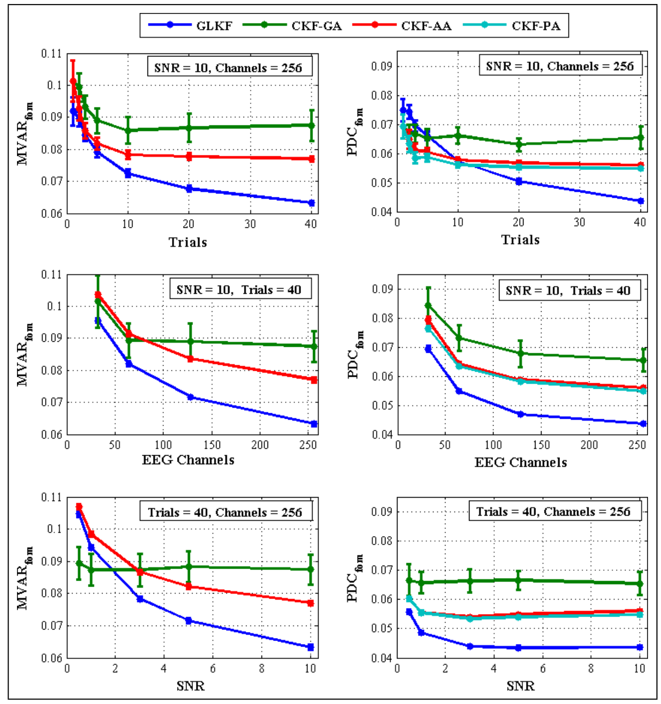

Fig. 2. Figures of merit ($\mathrm{MVAR_{fom}}$ and $\mathrm{PDC_{fom}}$) for different Kalman filter approaches at various levels of trials, EEG channels and SNR for TV-MVAR and TV-PDC estimation.

III. RESULTS

Each figure of merit was calculated compared to the theoretical values from the ground-truth model for different number of trials, number of EEG channels and SNR for each of the four possible Kalman filter approaches i.e. GLKF, CKF-GA, CKF-AA, CKF-PA.

Fig.2 shows the performance of different approaches on $\mathrm{MVAR_{fom}}$ and $\mathrm{PDC_{fom}}$ at various levels of the factors investigated. The bar on each plot indicates the standard deviation of the mean value computed across 50 realizations. Note that $\mathrm{MVAR_{fom}}$ for CKF-PA are not calculated since we used MVAR estimates of the individual trials. Based on one-way repeated measure ANOVAs for $\mathrm{MVAR_{fom}}$, the GLKF approach was significantly better in performance compared to the other methods when SNR >3 and number of trials >10. When SNR is low (≤ 1) CKF-GA performs best if the number of trials is not too low (> 5). Based on $\mathrm{PDC_{fom}}$, GLKF is significantly better in case the number of trials is high enough (> 10) and SNR > 1. When the number of trials is low (≤ 10) CKF-AA and CKF-PA showed superior performance when SNR > 1. In contrast to other approaches CKF-GA showed higher variance and no improved accuracy with increasing levels of SNR and number of trials. Interestingly, we also observed an improved performance when sources are reconstructed with an increasing number of EEG channels and this holds for each approach.

IV. DISCUSSION

The results obtained from the simulated data clearly indicated differences in the accuracy of the different Kalman filter approaches in TV-MVAR and TV-PDC estimation for multi-trial EEG or cortical source data.

Simulated data are often applied to study the effective connectivity [12], [20] directly at the level of sources or channels. However, we investigated the connectivity pattern at the level of cortical sources inversely re-estimated from the simulated EEG instead of the original sources. This provides a more realistic situation where accuracy of MVAR and TV-PDC estimation is evaluated after the source modeling which in itself may affect the accuracy.

GLKF showed the best performance among the possible Kalman filter approaches when SNR >3 and number of trials >10. These findings are consistent with a previous study in which it was shown that certain levels of SNR and number of trials were required for an accurate GLKF approach [12]. In addition to that, our study showed that in case the data contains a low number of trials, applying CKF-AA or CKF-PA can be an alternative to estimate TV-PDC. The exact levels of the factors when one method outperforms another, can not be determined based on this study because it may depend on many other factors like e.g. number of sources included in the analysis. However, this study gives some indication for the most suitable approach for the levels of the factors included. CKF-PA and CKF-AA showed similar performances, however given the higher computation time required for CKF-PA, the CKF-AA approach is preferred. In contrast to other approaches CKF-GA showed the worst performance when looking at TV-PDC. Averaging EEG data across trials may have disturbed the stochastic structure in the averaged data leading to an inferior accuracy. Indeed, a primary assumption of MVAR modeling is that each single trial is considered as a stochastic process [10]. This finding can be important for future studies performing TV-MVAR or TV-PDC estimation on averaged ERP data.

V. CONCLUSIONS

The results showed that the general linear Kalman filter (GLKF) is the best approach when the number of trials and SNR are sufficiently high. If this is not the case, a valid alternative is the classical Kalman filter approach in which time varying partial directed coherence is calculated from the average time varying multivariate autoregressive model parameters (CKF-AA). The accuracy of a classical Kalman filter approach applied on averaged EEG data across trials (CKF-GA) shows the worst performance in most cases.

REFERENCES

[1] J. Toppi, M. Petti, D. Mattia, F. Babiloni, and L. Astolfi, Time-Varying Effective Connectivity for Investigating the Neurophysiological Basis of Cognitive Processes, Neuromethods, vol. 91, pp. 171, 2015.

[2] K. Sameshima and L. A. Baccalá, Methods in Brain Connectivity Inference through Multivariate Time Series Analysis, CRC Press, 2014.

[3] D. W. Gow, and A. C. Nied, Rules from Words: A Dynamic Neural Basis for a Lawful Linguistic Process, PLoS One, vol. 9, no. 1, pp. e86212, 2014.

[4] M. Arnold, W. H. R. Miltner, H. Witte, R. Bauer, and C. Braun, Adaptive AR modeling of nonstationary time series by means of Kalman filtering. IEEE Trans. Biomed. Eng., vol. 45, no. 5, pp. 553, 1998.

[5] T. Milde, L. Leistritz, L. Astolfi, W. H. R. Miltner, T. Weiss, F. Babiloni, and H. Witte, A new Kalman filter approach for the estimation of high-dimensional time-variant multivariate AR models and its application in analysis of laser-evoked brain potentials, Neuroimage, vol. 50, no. 3, pp. 960, 2010.

[6] G. A. Giannakakis and K. S. Nikita, Estimation of time-varying causal connectivity on EEG signals with the use of adaptive autoregressive parameters, presented at Conf. Proc. IEEE Eng. Med. Biol. Soc., pp. 3512, Aug 2008.

[7] D. Tang, L. Hu, H. Li, Q. Zhang, and A. Chen, The neural dynamics of conflict adaptation within a look-to-do transition, PLoS One, vol. 8, no. 2, pp. 57912, 2013.

[8] K. Eftaxias, and S. Sanei, Diffusion adaptive filtering for modelling brain responses to motor tasks, presented at 18th Int. Conf. Digit. Signal Process., vol. 1, no. 1, July 2013.

[9] A. Omidvarnia, G. Azemi, B. Boashash, J. Otoole, P. Colditz, and S. Vanhatalo, Measuring time-varying information flow in scalp EEG signals: Orthogonalized partial directed coherence, IEEE Trans. Biomed. Eng. vol. 61, no. c, pp. 680, 2014.

[10] L. Hu, Z. G. Zhang, and Y. Hu, A time-varying source connectivity approach to reveal human somatosensory information processing, Neuroimage, vol. 62, no.1, 2012.

[11] L. Astolfi, F. Cincotti, D. Mattia, F. D. V. Fallani, A. Tocci, A. Colosimo, S. Salinari, M. G. Marciani, W. Hesse, H. Witte, M. Ursino, M. Zavaglia, and F.Babiloni, Tracking the Time-Varying Cortical Connectivity Patterns by Adaptive Multivariate Estimators, IEEE Trans. Biomed. Eng., vol. 55, no. 3, pp. 902, 2008.

[12] J. Toppi, F. Babiloni, G. Vecchiato, F. D. V. Fallani, D. Mattia, S. Salinari, T. Milde, L. Leistritz, H. Witte, and L. Astolfi, Towards the time varying estimation of complex brain connectivity networks by means of General Linear Kalman Filter approach, presented at Annu. Int. Conf. IEEE Eng. Med. Biol. Soc. EMBS, pp. 6192, 2012.

[13] L. A. Baccalá and K. Sameshima, Partial directed coherence: a new concept in neural structure determination, Biol. Cybern., vol. 84, no. 6, pp. 463, 2001.

[14] L. Astolfi, F. Cincotti, D. Mattia, M. G. Marciani, L. A. Baccala, F. V. D. Fallani, S. Salinari, M. Ursino, M. Zavaglia, and F. Babiloni, Assessing cortical functional connectivity by partial directed coherence: Simulations and application to real data, IEEE Trans. Biomed. Eng., vol. 53, no. 9, pp. 1802, 2006.

[15] S. Haykin, Kalman filtering and neural networks, Wiley Online Library, 2001.

[16] A. Schlögl, Time Series Analysis - A toolbox for the use with Matlab, 1996-2014.

[17] F. Tadel, S. Baillet, J. C. Mosher, D.Pantazis, and R. M. Leahy, Brainstorm: A user-friendly application for MEG/EEG analysis, Comput. Intell. Neurosci., vol. 2011, no. 1, pp. 45, 2011.

[18] C. Gillebert, D. Mantini, R. Peeters, P. Dupont, R. Vandenberghe, Cytoarchitectonic mapping of attentional selection and reorienting in parietal cortex, NeuroImage, vol. 67, no. 0, pp. 257, 2013.

[19] A. Gramfort, T. Papadopoulo, E. Olivi, and M. Clerc, Openmeeg: opensource software for quasistatic bioelectromagnetics, Biomed. Eng. Online, vol. 9, no. 1, pp. 45, 2010.

[20] L. Leistritz, B. Pester, A. Doering, K. Schiecke, F. Babiloni, L. Astolfi, and H. Witte, Time-variant partial directed coherence for analysing connectivity: a methodological study, Philos. Trans. A. Math. Phys. Eng. Sci., vol. 371, pp. 20110616, 2013.

[21] R. D. Pascual-Marqui, Standardized low-resolution brain electromagnetic tomography sLoreta: technical details, Methods Find. Exp. Clin. Pharmacol., vol. 24 Suppl D pp. 5, 2002.

[22] T. Schneider and A. Neumaier, Algorithm 808 ARfit-a matlab package for the estimation of parameters and eigenmodes of multivariate autoregressive models, ACM Trans. Math. Softw., vol. 27, no. 1, pp. 58, 2001.

[23] C. Porcaro, F. Zappasodi, P. M. Rossini, and F. Tecchio, Choice of multivariate autoregressive model order affecting real network functional connectivity estimate, Clin. Neurophysiol., vol. 120 no. 2, pp. 436, 2009.